Variographic analysis of public exposure to electromagnetic radiation due to cellular base stations

Thomas Lemaire[1]*, Joe Wiart[2], and Philippe De Doncker[1]

[1]Université Libre de Bruxelles (ULB), OPERA Department, Brussels, Belgium.

[2]Télécom ParisTech, LTI CNRS, Chaire C2M, Paris, France.

*Corresponding author : Thomas Lemaire, OPERA - Wireless Communications Group - CP 165/81, Université Libre de Bruxelles (ULB), Avenue F. Roosevelt 50, 1050 Brussels, Belgium. E-mail: tlemaire@ulb.ac.be.

Grant sponsor: Fédération Wallonie-Bruxelles.

Conflict of interest : none.

Abstract - The spatial structure of the vertical component of the electric field emitted by base stations in the Brussels Region (Belgium) is measured, and studied using the variogram. A relationship between the variogram shape and the base station antenna density in each measurement area is found: the variogram range and sill level are shown to depend on the BTS antenna density, following exponential laws.

Key words: Exposure assessment; Variographic analysis; Urban environment; Frequency Selective Measurements; Cellular Base Stations

Introduction

In the context of growing public concerns and scientific debates about possible adverse effects on human health of electromagnetic waves emitted by cellular base stations (BTS), the need for tools able to efficiently characterize the spatial distribution of the exposure is constantly rising. Classical exposure assessment around BTS is time consuming and often provides measurements in only a few distinct locations. However, for epidemiological surveys or for communication to the public, among other purposes, one might want to be able to establish a cartography of the exposure levels. To this aim, geostatistics provide numerous tools and methods to predict the value (or the probability that this value is whithin a certain range) of a spatially distributed random variable, given a limited set of samples and the knowledge of some statistical features of this random variable.

Previous works applied geostatistical methods to electromagnetic exposure assessment in urban areas. In De Doncker et al. [2006], spatial interpolation of the electric field using kriging was developed and tested in an indoor environment. In Azpurua and Dos Ramos [2010], three interpolation methods were compared for assessing the total electric field exposure in a urban area: splines, Inverse Distance Weighting (IDW) and kriging. The study concluded that IDW gave the best interpolation results. However, it should be noted that only kriging provides, besides interpolated values, an information about the uncertainty on these values. This feature makes kriging much more suited to applications where the probability that the exposure exceeds a given treshold is to be evaluated. In Isselmou et al. [2008], a method of interpolation based on kriging with external drift was proposed. The measures focused on the GSM900 signal, and were performed using a personal dosimeter. In Paniagua et al. [2013], a broadband electric field

probe (100 kHz - 3 GHz) was used to conduct extensive measurements in an urban area. The data were then used for kriging and the influence of the sampling resolution on the interpolation quality was studied. In Aerts et al. [2013a], the GSM900 field level was interpolated (with cubic splines) from a set of measurement samples which were selected *via* sequential design, and performed using a personal dosimeter. In Aerts et al. [2013b], the sequential design presented in Aerts et al. [2013a] was adapted to locate *hotspots* (small areas where the electric field level is significantly higher than the average), using kriging for interpolating the electric field and the related uncertainty (necessary for the sequential sampling design). The hotspots were located using a broadband electric field probe (100 kHz - 3 GHz), and the contribution of the different services to the total electric field was assessed using a spectrum analyzer.

No in-depth variographic analysis of the electric field emitted by BTS is yet available, however. Since modeling the variogram is the foundation of kriging, this is a significant lack in the field of Geostatistics applied to electromagnetic wave exposure assessment. In this context, the goal of this work is to provide a detailed variographic analysis of the general public exposure to electromagnetic waves emitted by BTS. Using a spectrum analyzer mounted on a car, geotagged samples of the electric field spectrum were taken over a frequency band covering the three telecommunication standards in the Brussels Region (GSM, UMTS, LTE). The advantage of frequency selective measurements over broadband measurements is that it allows one to isolate the signals coming from telecommunication BTS.

Materials and Methods

The measurements took the form of drive tests performed with a spectrum analyzer (FSH8, Rohde & Schwarz, Munich, Germany) in combination with a tri-axes calibrated antenna (TSEMF-B1, Rohde & Schwarz, Munich, Germany), range 30 MHz - 3 GHz, mounted on a moving car. The antenna was mounted in such a way that it was on the side of the car, just above the car roof level and 1.50 m above the ground. These drive tests were repeated in 8 different areas of the Brussels Region, selected to represent a variety of urban environments (residential, office areas...). The average number of floors for each area was between 1.68 and 4.23, and the BTS antenna density was between 1.06 and 28.81 antennas/km². The area diameter was roughly chosen between 1 km and 2 km. General properties (BTS density, average building height, ...) of the areas were available through databases from Bruxelles Environnement [2015] and IBSA [2015]. This size of measurement area offered a trade-off between being large enough to gather enough measurement samples and ensure that the variogram sill is reached, and small enough to be able to make the assumption that the general properties of the area can be considered stationary.

The spectrum analyzer was set up with a resolution bandwidth (RBW) of 3 MHz and a frequency span going from 600 MHz to 2490 MHz, covering the GSM, UMTS and LTE services in Brussels. The sweep time was chosen equal to 50 ms, and the root mean square (RMS) detector was used. A GPS receiver was used for geotagging of measurement samples, and the car was kept going at a speed of 30 km/h maximum. With these settings, the sampling period of the measured electric field was 275 ms (sweep time + data acquisition), which gives a distance of 2.3 m maximum between two samples. Since the GPS acquisition rate is much slower (1 s between each sample), the GPS coordinates were interpolated between the acquired samples.

Only the vertical component of the electric field has been measured: when using the R&S TSEMF-B1 in tri-axes mode, each component is measured in turn via an internal switch. Since the three components are not measured simultaneously and the measuring device is moving, each measured component would correspond to a different location. For this reason, it was chosen to focus on the vertical polarization of the electric field. The outcomes of the geostatistical analysis will then also describe the spatial distribution of the electric field's vertical component only, but since the measured electric field is originating from several BTS having various polarizations, one should expect that the methodology presented here could be applied to the other polarizations, or to the combination of the three of them.

The physical quantity that was considered is the 900 MHz equivalent of the total electric field, *i.e.*:

$$E_{900} = \sqrt{\sum_{f=10MHz}^{300GHz} \left(\frac{E_f}{E_{L,f}} E_{L,900MHz}\right)^2}$$

with E_f the field level measured at frequency f, $E_{L,f}$ the electric field strength reference level for general public exposure at frequency f as defined by the International Commission on Non-Ionizing Radiation Protection (ICNIRP [1998]), and $E_{L,900MHz}$ = 41.25 V/m. This value is convenient for assessing exposure compliance with ICNIRP guidelines, as well as with local legislations, since the exposure limits in the Brussels Region [Moniteur Belge, 2014] are simply taken as a fraction of the ICNIRP limits: a value lower than 41.25 V/m for E_{900} will ensure that ICNIRP guidelines are satisfied, while a value lower than 6 V/m is required by regulations in the Brussels Region.

In the sum, only the E_f corresponding with GSM, UMTS and LTE signals emitted by

base stations (downlink) were taken into account.

For each measurement area, the experimental isotropic variogram of the total electric field level has been computed. The experimental isotropic variogram $\hat{\gamma}(h)$ is given by [Chilès and Delfiner, 2012; Leuangthong et al., 2008]:

$$\hat{\gamma}(h) = \frac{1}{2} \underset{|\vec{h}|=h}{mean}[\{z(\vec{x}) - z(\vec{x}+\vec{h})\}^2] \quad (1)$$

where $\vec{x}$ is the position of the samples and z the random variable under study (in the present case, the 900 MHz equivalent of the total electric field, defined above). It gives half the value of the variance of z between each pair of samples separated by a distance h. The isotropic variogram $\hat{\gamma}(h)$ is a particular case of the general expression of the variogram $\hat{\gamma}(\vec{h})$ where the variance is evaluated for each pair of samples separated by a spatial vector $\vec{h}$. The assumption was made that the number of base stations contributing to the measured field level within the measurement area is large enough to consider that the variance between samples separated by a vector $\vec{h}$ does not depend of the direction of $\vec{h}$.

The choice of the spatial sampling pattern is crucial, and has experienced several changes in the successive adjustments of the measurement procedure. The following measurement strategy has finally been selected: the electric field is measured along transects, *i.e.* straight lines, formed by long straight streets (or as straight as practically possible) cutting the measurement area. Transects are chosen as long as possible for the considered measurement area, to ensure that the variogram sill is reached, while being evenly distributed among the area to give a good enough representation of the spatial structure of the electric fiald in the whole area.

The experimental variogram for one measurement area is then computed as follows: the squared difference of E_{900} is computed only for pairs of samples located in the same transect, and then the mean of these squared differences is computed over the whole set of sample pairs (*i.e.* belonging to any transect) for a given h. With T representing a transect, expression (1) becomes:

$$\hat{\gamma}(h) = \frac{1}{2} \underset{\substack{|\vec{h}|=h \\ \vec{x},\vec{x}+\vec{h}\in T}}{mean}[\{z(\vec{x}) - z(\vec{x}+\vec{h})\}^2] \quad (2)$$

Results

In Figure 1, the cumulative distribution function (CDF) of the 900 MHz equivalent of the total electric field is shown.

The measured 900 MHz equivalent of the total electric field E_{900} follows a lognormal distribution law. The normal distribution fitting the CDF of E_{900} expressed in dBµV/m has a mean value equal to 105.5 dBµV/m and a variance equal to 8.07 dBµV/m. Its 95th percentile is equal to 118.3 dBµV/m (0.82 V/m). The probability that E_{900} is above the ICNIRP reference level of 41.25 V/m at 900 MHz is about 2×10^{-9}, and the probability that it is above the maximum authorized public exposure in the Brussels Region of 6 V/m is about 8×10^{-5}.

In Figure 2, the experimental variogram computed for one of the eight measurement areas is displayed. It corresponds to a residential area, with shops, in a reasonably dense part of the city (average number of floors of buildings = 2.96, BTS antenna density = 17 antennas/km²). The other variograms all display the same general aspect: a linear growth near the origin, a

negative curvature appearing as the distance h increases, and finally a constant sill for h higher than a distance called the range of the variogram. This area was chosen as an illustration because its range and sill level have average values among the measurement areas.

The variogram is actually truncated after the displayed plot. Indeed, for higher values of h, less and less pairs of samples are available for the computation of $\hat{\gamma}(h)$, and the variogram begins to show an erratic behaviour, which is usually the case when the h bin size is uniform.

Discussions

The spherical model has been found to best fit the experimental variograms:

$$\gamma(h) = \begin{cases} c\{\frac{3h}{2a} - \frac{1}{2}(\frac{h}{a})^3\} + n & h \le a \\ c + n & h > a \end{cases}$$

where a is the range of the variogram, and c the level of the sill [Webster and Oliver, 2007]. A *nugget* term n has been added, representing the non zero value of the variogram near the origin (due to a discontinuous measured field level).

The variogram range a given by the spherical model for each of the experimental variograms is plotted in Figure 3 as a function of the BTS antenna density in the corresponding measurement area. Of all the relevant area parameters available to the authors (BTS antenna density, population density, average number of floor of buildings, office density) this one gives the clearest dependency with the variogram range.

This can be easily understood: as the antenna density increases, the cell pattern repeats itself with a higher spatial frequency and pairs of samples become more likely to belong to different cells even when relatively close to each other. The distance for which their electric

field values are uncorrelated thus decreases: the variogram range is reached sooner.

An exponential regression was fitted to the set of data points in order to model the dependency between the variogram range a and the antenna density A. This model gives a good representation of the observed trend in the considered range of points, but could be expected to diverge as A approaches 0.

The equation for this exponential model is:

$$a = 863.7e^{-0.078A}$$

where the range a is expressed in meters and the antenna density A in [antennas/km²]. The standard deviation around the regression is $\sigma = 134.01\,\text{m}$.

The variogram sill level is plotted in Figure 4 as a function of the BTS antenna density in each measurement area. It is clear that again, a dependency exists between the two variables. This can be explained by the fact that when the antenna coverage is more dense, the path loss between the surrounding antennas and the measurement point is in average lower than when the antenna coverage is more sparse. The average squared difference between high and low values of the field level is thus lower, even for pairs of samples further apart than the variogram range.

The regression model selected to express the dependency between the variogram sill level and the antenna density is again an exponential model, with equation:

$$c = 94.88e^{-0.064A}$$

with c the variogram sill level in (dBµV/m)² and A the antenna density in [antennas/km²]. The standard deviation around the regression is $\sigma = 16.03\,(\text{dB}\mu\text{V/m})^2$.

It should be noted that for both the range and the sill level of the variograms, a

dependency with the average number of floors could be observed, very similar to the one with the antenna density. However, these two variables cannot be considered as independent variables for our model, since the average number of floors and the antenna density appear to be strongly correlated in the areas where the measurements were made, as it is shown in Figure 5. The linear regression shows that the antenna density A depends on the average number of floors F as:

$$A = 10.31F - 18.46$$

Because of this strong correlation between the two variables, considering the variogram sill and range as a function of the two of them instead of only one does not add much information, and the antenna density was chosen as the variable to model the variogram sill and range since it provides a clear interpretation as explained above.

No relationship between the nugget effect term n and any of the area parameters could be found. This is no surprise, since the nugget effect is inherent to small scale variations in the measured values and should then not be linked to larger scale effects. The nugget term n was thus chosen to be modeled simply by its mean value:

$$\mu_n = 6.87 \text{ (dBμV/m)}^2$$

The minimum and maximum values for n in the variograms were respectively 1.22 (dBμV/m)² and 13.50 (dBμV/m)².

Conclusions

The measurement method described here enabled to establish variogram models well suited for future prediction purposes, and provides a standard procedure that is repeatable in

other urban areas. In the Brussels Region, the 900 MHz equivalent of the total electric field was shown to follow a lognormal distribution with a mean of 105.5 dBμV/m and a variance of 8.07 dBμV/m. A spherical model was fitted to the experimental variograms, for which the range and sill were shown to depend on the BTS antenna density in the region where the measurements took place. This dependency was modeled by exponential laws, which would allow one to obtain a model for the variogram of the 900 MHz equivalent electric field, in any area where the BTS antenna density is known.

Acknowledgements

The authors wish to thank Fédération Wallonie-Bruxelles for funding this study through the BWARE project (Brussels-Wallonia Auxiliary Radiators for Exposure reduction), as well as the Bruxelles Environnement institute (IBGE) for providing the data used to extract the BTS antenna density.

References

Aerts S, Deschrijver D, Joseph W, Verloock L, Goeminne F, Martens L, Dhaene T. 2013. Exposure assessment of mobile phone base station radiation in an outdoor environment using sequential surrogate modeling. Bioelectromagnetics 34:300–311.

Aerts S, Deschrijver D, Verloock L, Dhaene T, Martens L, Joseph W. 2013. Assessment of outdoor radiofrequency electromagnetic field exposure through hotspot localization using kriging-based sequential sampling. Environmental Research 126:184–191.

Azpurua M, Dos Ramos K. 2010. A comparison of spatial interpolation methods for

estimation of average electromagnetic field magnitude. Progress In Electromagnetics Research M 14:135–145.

Bruxelles Environnement. 2015. Carte des antennes émettrices. Available from: http://www.environnement.brussels/thematiques/ondes-et-antennes/ou-sont-les-antennes/carte-des-antennes-emettrices [French, last accessed 19 Jan 2016].

Chilès J-P, Delfiner P. 2012. Geostatistics, Modeling Spatial Uncertainty. Second edition. Hoboken, New Jersey: John Wiley & Sons.

De Doncker Ph, Dricot J-M, Meys R, Hélier M, Tabbara W. 2006. Electromagnetic fields estimation using spatial statistics. Electromagnetics 26:111–122.

IBSA (Institut Bruxellois de Statistique et d'Analyse). 2015. Le monitoring des quartiers de la région de bruxelles-capitale. Available from: https://monitoringdesquartiers.irisnet.be/ [French, last accessed 19 Jan 2016].

ICNIRP (International Commission on Non-Ionizing Radiation Protection). 1998. Guidelines for limiting exposure to time-varying electric, magnetic, and electromagnetic fields (up to 300 ghz). Health Physics 74(4):494–594.

Isselmou Y O, Wackernagel H, Tabbara W, Wiart J. 2008. Geostatistical estimation of electromagnetic exposure. geoENV VI:59–70.

Leuangthong O, Khan K D, Deutsch C V. 2008. Solved Problems in Geostatistics. Hoboken, New Jersey: John Wiley & Sons.

Moniteur Belge. 3 Apr 2014. Ordonnance modifiant l'ordonnance du 1er mars 2007 relative à la protection de l'environnement contre les éventuels effets nocifs et nuisances provoqués par les radiations non ionisantes et modifiant l'ordonnance du 5 juin 1997 relative

aux permis d'environnement. Available from: http://www.ejustice.just.fgov.be/cgi_loi/change_lg.pl?language=fr&la=F&cn=2014040316&table_name=loi [French, last accessed 27 Apr 2016].

Paniagua J M, Rufo M, Jimenez A, Antolin A. 2013. The spatial statistics formalism applied to mapping electromagnetic radiation in urban areas. Environmental Monitoring and Assessment 185:311–322.

Webster R, Oliver M A. 2007. Geostatistics for Environmental Scientists. Second edition. Hoboken, New Jersey: John Wiley & Sons.

Figures

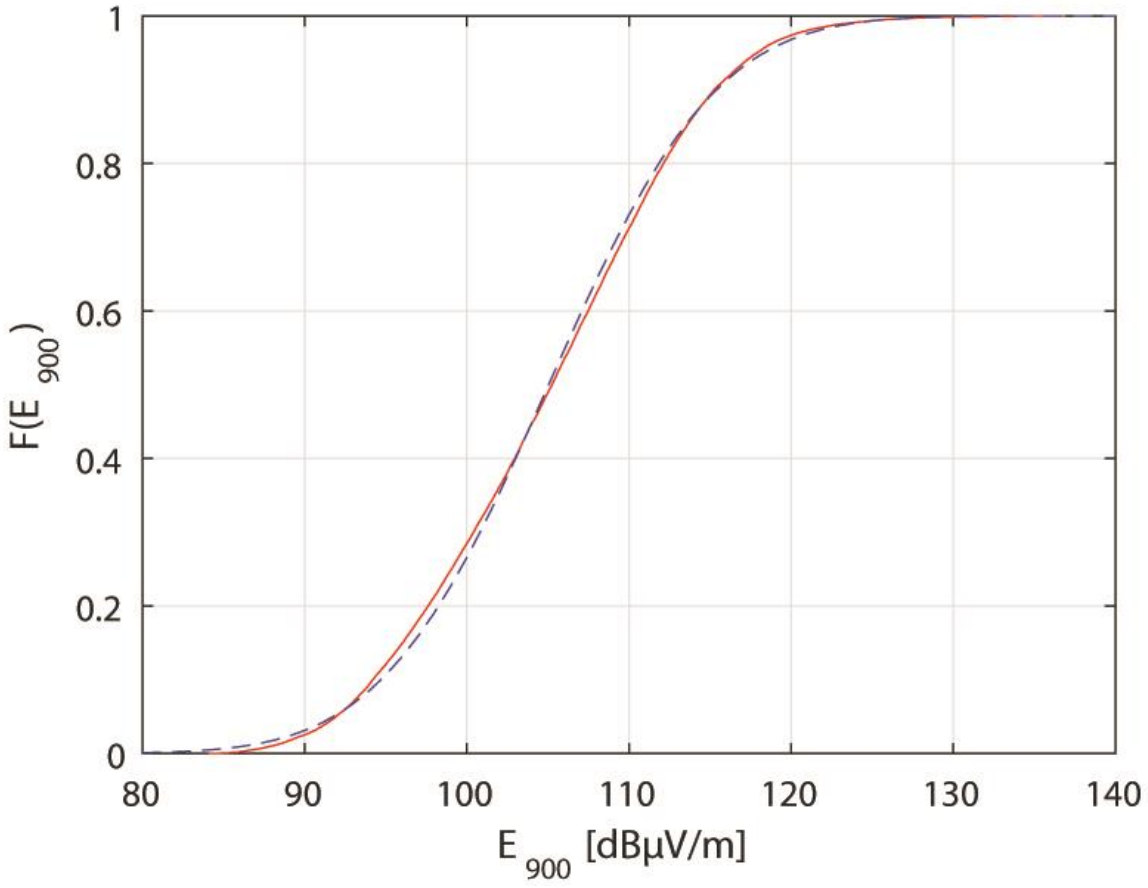

Figure 1: Cumulative distribution function of the total electric field level 900 MHz equivalent over the different measurement areas (solid line). Normal regression (dashed line).

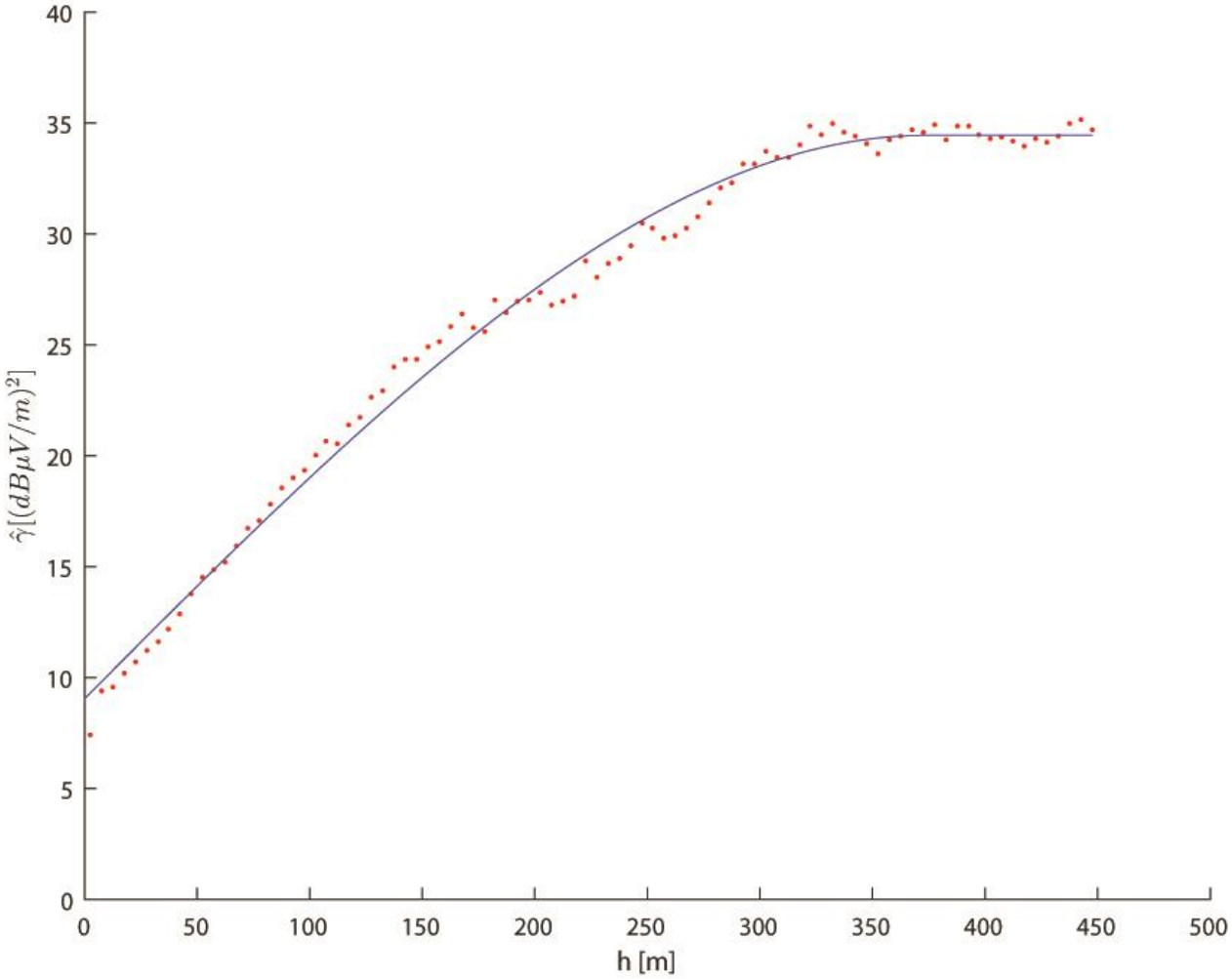

Figure 2: Experimental variogram of the measured 900 MHz equivalent of the total electric field, for one of the eight measurement areas (dots). Spherical model fit (solid line).

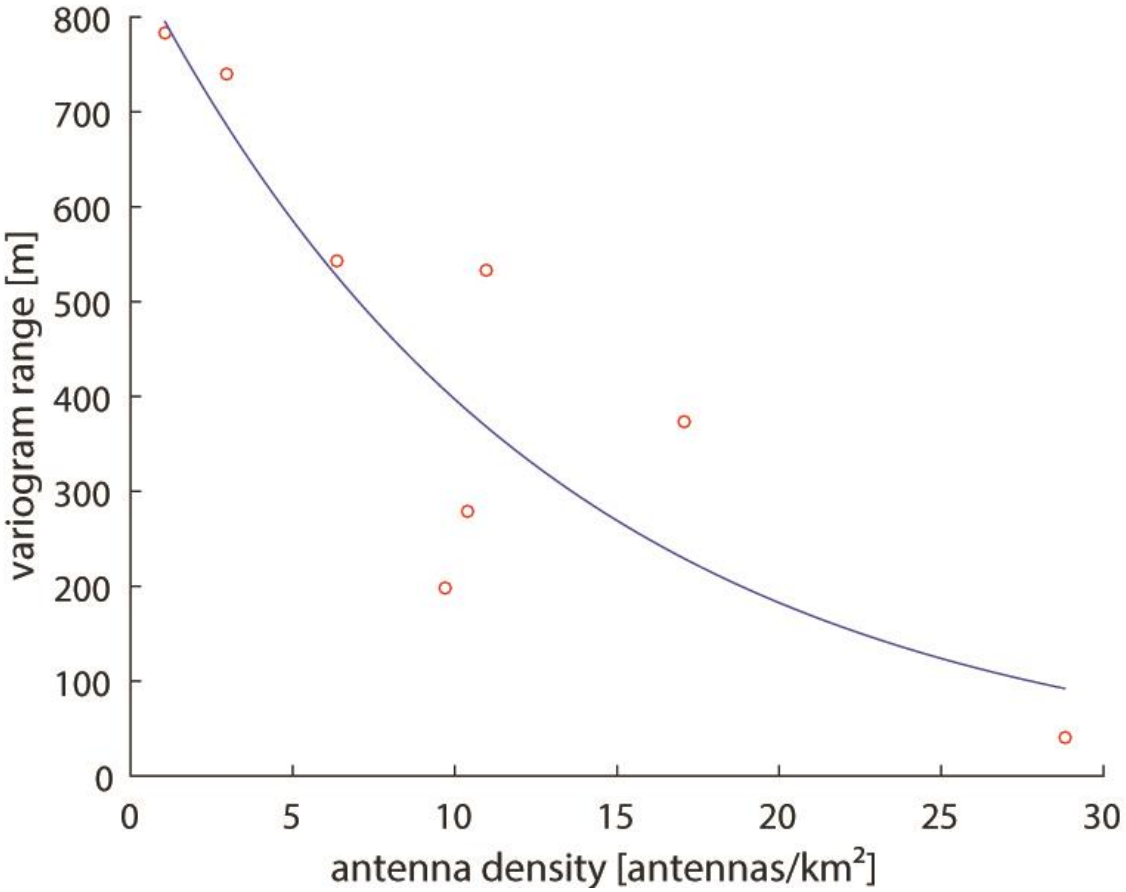

Figure 3: Experimental variogram range a (spherical model) as a function of the antenna density in the measurement area (circles). Exponential regression (solid line).

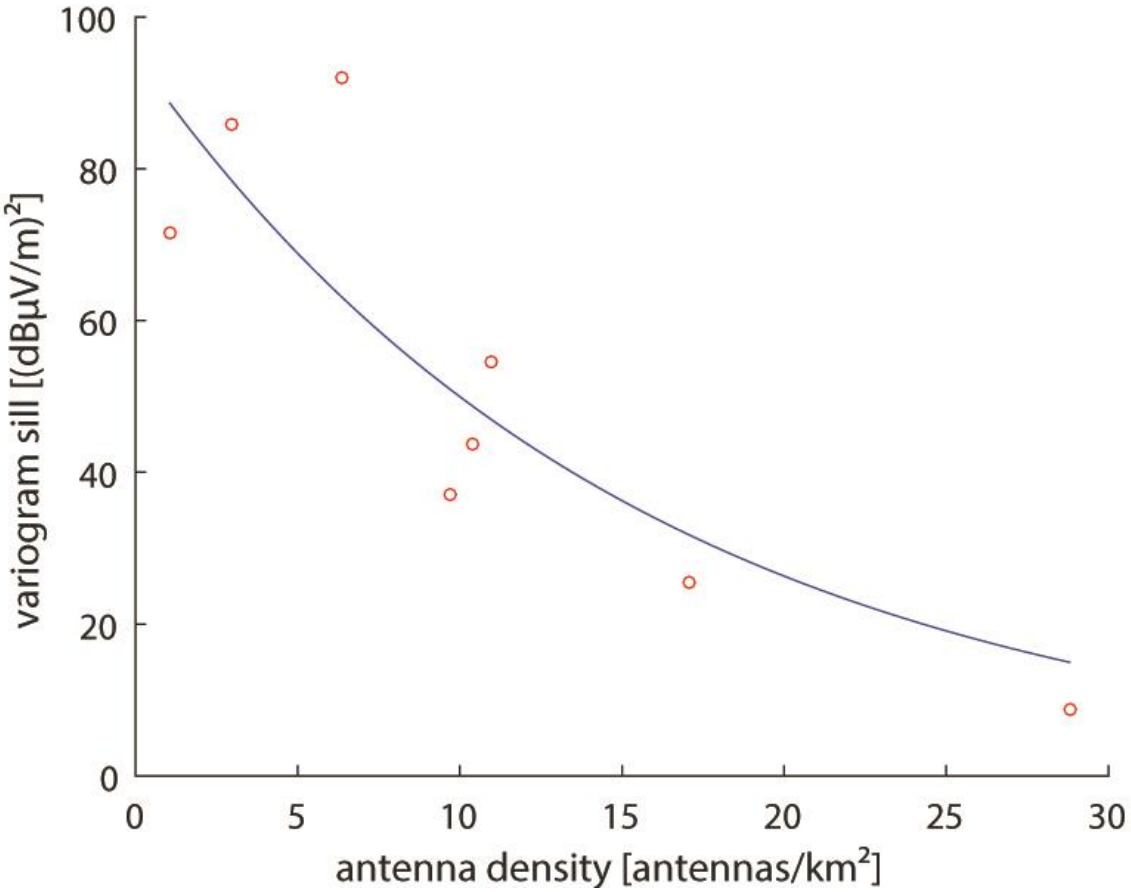

Figure 4: Experimental variogram sill level c (spherical model) as a function of the antenna density in the measurement area (circles). Exponential regression (solid line).

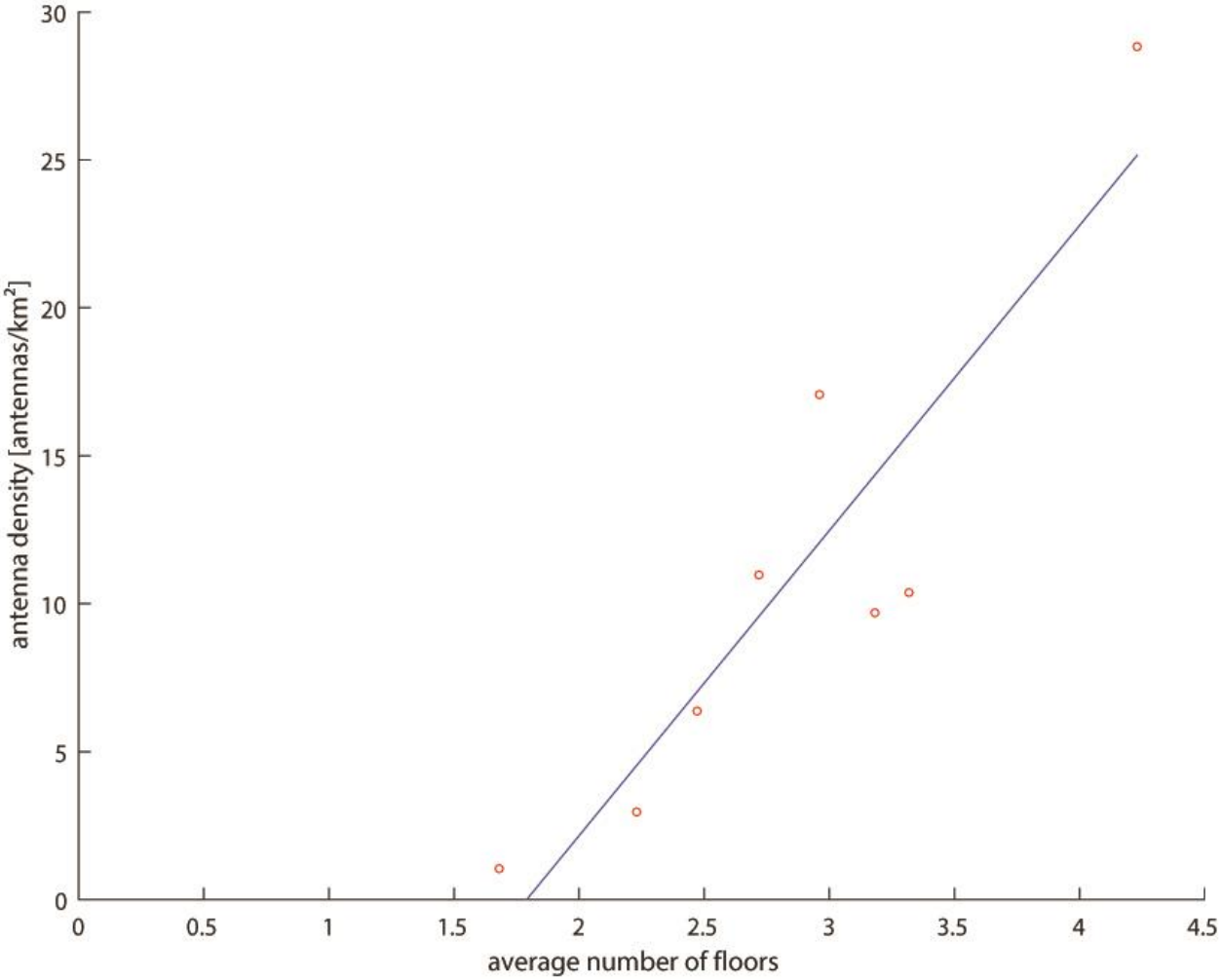

Figure 5: Antenna density in the measurement area as a function of the average number of floors (circles). Linear regression (solid line).